surfaces

MDPI

Article

Surface Characteristics and Performance Optimization of W-Doped Vanadium Dioxide Thin Films

Chuen-Lin Tien [1,2,*], Chun-Yu Chiang [2], Jia-Kai Tien [3], Ching-Chiun Wang [4] and Shih-Chin Lin [4]

[1] Department of Electrical Engineering, Feng Chia University, Taichung 40724, Taiwan
[2] Ph.D. Program of Electrical and Communications Engineering, Feng Chia University, Taichung 40724, Taiwan; hank4681898@gmail.com
[3] Graduate Institute of Library & Information Science, National Chung Hsing University, Taichung 402202, Taiwan; tienalex020290@gmail.com
[4] Mechanical and Systems Research Lab, Industrial Technology Research Institute, Hsinchu 310401, Taiwan; juin0306@itri.org.tw (C.-C.W.); shihchin@itri.org.tw (S.-C.L.)
* Correspondence: cltien@fcu.edu.tw; Tel.: +886-4-2451-7250 (ext. 3809)

Abstract: This study explores the surface characteristics evaluation and performance optimization of tungsten (W)-doped vanadium dioxide (VO_2) thin films. W-doped vanadium dioxide films were deposited on B270 glass substrates using an electron beam evaporation technique combined with the ion beam-assisted deposition (IAD) method. The Taguchi method was used to analyze the performance optimization of VO_2 thin films, and L_{16} orthogonal array design and Minitab software were used for optimization calculations. The surface roughness, visible light transmittance, infrared transmittance, and residual stress of un-doped and tungsten-doped (3–5%) VO_2 thin films are set as the quality performance indicators of thin films. The goal is to identify the key factors that affect the performance of VO_2 thin films during deposition and optimize their process parameters. The experimental results showed that a VO_2 thin film with 3% tungsten doping, an oxygen flow rate of 60 sccm, a heating temperature of 280 °C, and a film thickness of 60 nm exhibited the lowest surface roughness of 2.12 nm. A VO_2 thin film with 5% tungsten doping, an oxygen flow rate of 0 sccm, a heating temperature of 280 °C, and a film thickness of 60 nm had the highest visible light transmittance at 64.33%. When the oxygen flow rate was 60 sccm, the heating temperature was 295 °C, the film thickness was 150 nm, and the tungsten doping was 5%, the VO_2 thin film showed the lowest infrared transmittance of 31.34%. A thin film with 5% tungsten doping, an oxygen flow rate of 20 sccm, a heating temperature of 265 °C, and a film thickness of 120 nm exhibited the lowest residual stress of −0.195 GPa.

Keywords: vanadium dioxide; thin film; Taguchi method; surface roughness; residual stress

Citation: Tien, C.-L.; Chiang, C.-Y.; Tien, J.-K.; Wang, C.-C.; Lin, S.-C. Surface Characteristics and Performance Optimization of W-Doped Vanadium Dioxide Thin Films. *Surfaces* **2024**, *7*, 1109–1124. https://doi.org/10.3390/surfaces7040073

Academic Editor: Gaetano Granozzi

Received: 2 November 2024
Revised: 3 December 2024
Accepted: 18 December 2024
Published: 20 December 2024

1. Introduction

The application of thin films has grown exponentially, becoming an indispensable part of industrial and research processes. Thin-film deposition can enhance surface properties such as wear resistance, corrosion resistance, fatigue, hardness, and other surface-related characteristics, making thin-film materials versatile and applicable across various industries. As a result, the production of high-quality optical thin films has become a crucial issue today. Vanadium dioxide-based films are used as smart windows, which can adjust the optical properties of windows according to the ambient temperature, regulate indoor solar radiation, and reduce the unnecessary energy consumption of air conditioning in buildings [1,2]. Its reversible metal-to-insulator transition near room temperature has garnered significant attention, making it a highly promising energy-saving material for smart windows [3,4]. Due to its ability to automatically adjust solar radiation based on external conditions, VO_2 thin films offer a solution to the looming energy crisis [5,6]. Currently, many methods have been used to fabricate VO_2 thin films [7–12], among which

the thin-film layer deposited by the physical vapor deposition (PVD) technique exhibits functional effects that improve component uniformity, adhesion, and durability, extend service life, and is suitable for mass production, thus enhancing product value [13]. The optimized combination of VO_2 thin-film parameters is essential for preparing single-layer or multi-layer composite thin films for smart window applications.

Vanadium dioxide has a phase transition temperature of 68 °C and is one of the most representative thermochromic materials [14]. At different temperatures, VO_2 undergoes a phase change that alters its structure, leading to variations in its optical properties. Due to its exceptional electro-optical modulation properties, high transmittance, and solar modulation capabilities, VO_2 is widely used in smart windows [15]. Energy consumption in buildings (air conditioning, heating, and lighting) accounts for 30–40% of global annual energy use, making energy efficiency and carbon reduction in this field an attractive topic [16]. Vanadium oxides (VO_x) exhibit 14 oxidation states and are highly sensitive to temperature. Each oxidation state of Vox presents distinct optical, electrical, and magnetic characteristics, as well as unique physical properties [17]. Among these, VO_2 undergoes a metal–insulator transition (MIT) at 68 °C, a temperature closest to room temperature, enabling tunable near-infrared (NIR) transmittance. However, the phase transition temperature (Tt) of VO_2 remains relatively high for energy applications related to ambient conditions [18]. To address this, research has focused on lowering the phase transition temperature through metal ion doping. It has been reported that doping with different elements can effectively modulate the phase transition temperature of VO_2 thin films [19]. Doping with ions higher than tetravalent (such as Nb^{6+}, Mo^{6+}, T^{a5+}, W^{6+}), and non-metallic ions (such as F^{-}) has been found to reduce the phase transition temperature of VO_2. When these ions replace the tetravalent vanadium ions, excess electrons are introduced into the d-electron orbitals of vanadium, leading to a reduction in the energy bandgap and, consequently, a decrease in the phase transition temperature. On the other hand, it has also been found that doping with ions lower than tetravalent (such as Ga^{3+}, Al^{3+}, Cr^{3+}) creates vacancies in the lattice, generating V_{5+} ions, which increase structural stability and raise the phase transition temperature [20].

Different research results have been obtained on how doping levels affect the phase transition temperature of VO_2 thin films. In some cases, an increase in the doping level leads to a decrease in the phase transition temperature, possibly due to the introduction of additional electrons that alter the material's electronic band structure and electron density. Liang [21] synthesized 2 at.% W-doped VO_2 composite films using the sol–gel method, reducing the phase transition temperature to 32 °C and achieving a solar modulation rate (ΔT sol) of 9.1%. Pan [22] used an organic sol–gel method to dope VO_2 films with 20 at.% W, reducing the phase transition temperature from 62.3 °C to 56 °C. However, this indicates that excessive W doping may introduce issues, as excess W atoms could precipitate at the grain boundaries, thereby not only reducing the phase transition effect of VO_2 but also adversely affecting its structure. Ji et al. [23] reported that VO_2 thin films with reduced phase transition temperatures were prepared via a hydrothermal synthesis method by adjusting the tungsten doping ratio. When the tungsten doping level was 1.7 at.%, the phase transition temperature dropped from 67.2 °C to 43.2 °C. These studies collectively demonstrate that tungsten-doped VO_2 can effectively modulate the phase transition temperature, further confirming that W-doped VO_2 films exhibit significant thermochromic performance enhancements.

It can be seen from the above literature discussion that there are many articles on the phase change characteristics and process methods of thermochromic VO_2 thin films, but there are few studies on the impact of process conditions on optimizing the performance of VO_2 thin films. Therefore, this study proposes the surface characteristic evaluation and performance optimization of W-doped VO_2 thin films based on the Taguchi method. First, the research process is established as the basis for factor selection and level setting, the orthogonal parameters of the table are designed and tested, and then W-doped VO_2 thin films are prepared using ion-assisted electron beam evaporation technology. Various

property evaluations and optical measurements are performed on the un-doped and W-doped VO_2 thin films. Finally, statistical analysis and optimization are performed on each measurement value to obtain the best process parameters.

2. Materials and Methods

2.1. Experimental Design

In the design and fabrication of optical thin films, designers must accurately understand the optical constants, such as the refractive index and extinction coefficient, along with the film thickness, to ensure that the final product meets the design specifications. Typically, the properties of materials in thin-film form differ significantly from their bulk material counterparts [24]. These material properties are closely related to the deposition method and coating conditions, including deposition temperature, pressure, deposition rate, substrate pretreatment, and other factors. These parameters play a crucial role in determining the final optical properties of the thin films. Therefore, precise control of these variables is key to achieving high-quality optical thin films. Our research focuses on improving the quality of thin film components, reducing production costs, and enhancing product competitiveness, and we often use the Taguchi method to optimize process parameters.

This method is highly effective in reducing experimental costs and accelerating development, utilizing formulas such as "Larger-the-Better", "Smaller-the-Better", and signal-to-noise ratios (S/N ratios) to identify the optimal parameter combinations and ensure successful experiments [25–27]. In the Taguchi method, the selection of control factors relies not only on the literature and expert experience but may also require preliminary screening tests to identify the most important factors. This ensures the precision of experimental design, leading to improved product quality and production efficiency.

2.2. Thin-Film Deposition

In this study, we utilized a SHOWA electron beam evaporation system (SGC-22SA, Showa Shinku, Japan) combined with ion beam-assisted deposition (IAD) to fabricate both un-doped and tungsten (W)-doped vanadium dioxide (VO_2) thin films. Four different vacuum pump systems were used to ensure an effective and stable vacuum process. Initially, an oil rotary pump and a mechanical booster pump were employed for the initial evacuation, which rapidly removed gasses from the system and reduced the pressure to the desired range. Subsequently, a diffusion pump and a cryopump were used to achieve a high-vacuum environment, ensuring stable deposition conditions. The electron gun was set to a maximum output power of 10 kW, with an operating voltage of 10 kV and a current of 1 A. These parameters were chosen to ensure that the thin-film materials were evaporated and deposited at a stable and uniform rate while maintaining energy input stability during the deposition process, thereby achieving high-quality film deposition results.

The thin films were deposited on 1-inch B270 circular glass substrates. Key parameters, such as gas flow rate, heating temperature, deposition time, and film thickness, were adjusted to explore the optimal conditions for VO_2 thin films. Based on prior research, the literature reviews, and empirical rules, we established the parameter levels for this study. The experimental factors included oxygen flow rate, heating temperature, film thickness, and the doping ratio of tungsten in the vanadium dioxide material. In other words, there are four key factors that affect film growth. For example, heating temperature will affect the microstructure and surface profile of the film; VO2 with different tungsten doping contents adjusts the phase transition temperature and improves the performance of the thermochromic thin film; oxygen flow affects the uniformity and phase transition stability; film thickness mainly affects the surface roughness and residual stress. Each factor was assigned four levels, as shown in Table 1. We used the L_{16} (4^4) orthogonal array, with four control factors and four levels for each, conducting 16 experiments based on the Taguchi L16 orthogonal table, as shown in Table 2. The aim was to optimize the process parameters for the electron beam evaporation of VO_2 thin films, ensuring that the films deposited

on B270 glass substrates exhibited high transmittance, low infrared transmittance, low residual stress, and low surface roughness. Through this optimization of VO_2 thin-film parameters, we aim to enhance the durability and transmittance of multi-layer composite films for smart window applications [25,26].

Table 1. Control factors with different levels.

Factor	Experimental Control Factors	Levels of Factor			
		1	**2**	**3**	**4**
A	O_2 flow rate (sccm)	0	20	40	60
B	Substrate temperature (°C)	250	265	280	295
C	Film thickness (nm)	60	90	120	150
D	W content ratio (%)	0	3	4	5

Table 2. Orthogonal array L_{16} (4^4) for VO_2 experimental samples.

Test Number	Factory (Level)			
	O_2 Flow Rate (sccm)	**Substrate Temperature (°C)**	**Film Thickness (nm)**	**W-Doped VO_2 Ratio (%)**
1	0	250	60	0
2	0	265	90	3
3	0	280	120	4
4	0	295	150	5
5	20	250	90	4
6	20	265	60	5
7	20	280	150	0
8	20	295	120	3
9	40	250	120	5
10	40	265	150	4
11	40	280	60	3
12	40	295	90	0
13	60	250	150	3
14	60	265	120	0
15	60	280	90	5
16	60	295	60	4

2.3. Measurement Methods

In the thin-film measurements conducted in this study, we utilized a UV–visible spectrophotometer (Shimadzu UV-2600i, Kyoto, Japan) to measure the transmittance of the materials. This instrument provides transmission spectral data versus wavelength data by analyzing the incident light of different wavelengths. The system is equipped with diffraction gratings to reduce stray light and avoid absorption errors. The system is also equipped with a high-sensitivity photomultiplier tube (PMT) detector, significantly expanding the linear measurement range. The specific wavelength range measured by this spectrophotometer is from 200 nm to 1000 nm. By analyzing the transmission spectrum using the envelope method [28,29], we can calculate the film's optical constants, which is a widely accepted and convenient method [30].

For infrared transmission spectra measurements of the thin films, we used a Fourier-transform infrared spectrometer (FTIR) (Model Nicolet iS5, Thermo Fisher Scientific, MA., USA) covering the measurement range of 7800 cm^{-1} to 350 cm^{-1}. An advantage of FTIR is its simple structure, with the moving mirror in the interferometer being the only mobile component, significantly reducing the likelihood of mechanical failure and making the overall maintenance straightforward and convenient.

The surface roughness of the films was evaluated using a homemade Linnik microscopic interferometer, utilizing a helium–neon laser (wavelength of 632.8 nm) as the light

source, as shown in Figure 1. The system was equipped with two 50× objectives, a two-axis translation stage, and a CCD camera for capturing high-resolution images of the sample surfaces. The system is enhanced with a self-developed MATLAB program that uses the fast Fourier-transform (FFT) algorithm for comprehensive image analysis [31]. The coherent laser beam, emitted from the helium–neon source, passed through a spatial filter and collimating lens to produce a plane wavefront. The light was then split into two beams by a beam splitter: one reflected from a reference mirror (with a flatness of λ/20) after passing through the first 50× objective, and the other reflected from the test sample surface after passing through the second 50× objective. The two reflected beams were recombined at the beam splitter, producing an interference pattern on the image plane, which was captured by the high-resolution CCD camera. The interference pattern was analyzed using the MATLAB program based on FFT, allowing the precise detection of surface height variations. Additionally, a digital Gaussian filter was applied to determine the cutoff wavelength of the signal, separating the high-frequency surface signal from the overall low-frequency surface profile. This method produced a 3D surface profile of the thin films, and surface roughness values were calculated by numerical method. A detailed description of the hardware architecture can be found in our previously published papers [32,33].

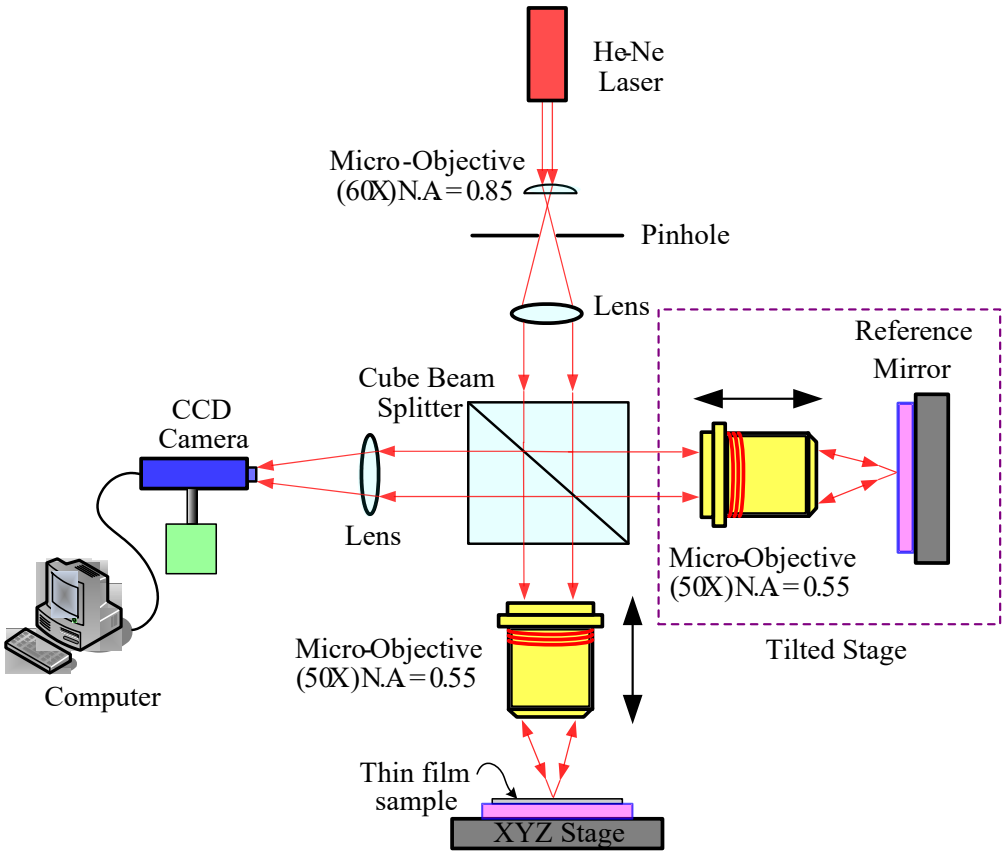

Figure 1. Schematic of a homemade Linnik microscopic interferometer.

The residual stress in thin films was measured by a homemade Twyman–Green interferometer combined with the FFT analysis [34–36]. A schematic diagram of this setup is shown in Figure 2. In the residual stress measurement process, a combination of a helium–neon laser with a micro-objective lens and pinhole was used to generate a precise point light source. The laser beam, after passing through a collimating lens, formed a plane wavefront. A beam splitter then divided the wavefront's amplitude, producing reflected and transmitted beams. These beams passed through the reference mirror (with a flatness of λ/20) and the test substrate, respectively. The two reflected beams were recombined at the beam splitter to generate an interference pattern, which was recorded by a digital

CCD camera. To calculate the residual stress in thin films, we used a self-developed stress analysis program that can accurately evaluate the residual stress in thin films [36,37].

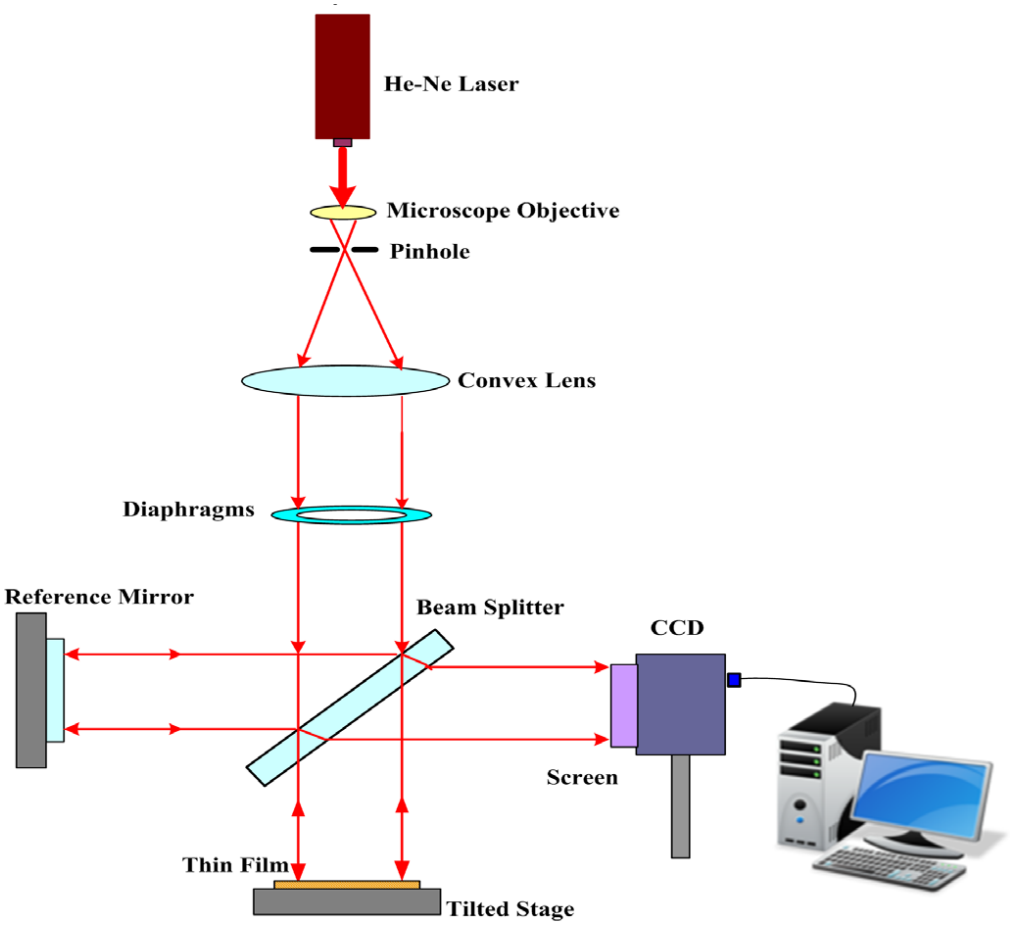

Figure 2. Schematic of a homemade Twyman–Green interferometer.

2.4. Signal-to-Noise Ratio

The Taguchi method employs orthogonal arrays to reduce variance and optimize process parameters. In the Taguchi method, the signal to noise (S/N) ratio is used as a performance characteristic to measure process robustness and to evaluate deviation from desired values [38]. The S/N ratio, a logarithmic function, is computed by assessing the proportion of signal (mean) to the noise (standard deviation). The signal-to-noise ratio is a logarithmic function. It is calculated by evaluating the signal ratio (average value) to noise (standard deviation). The experimental value is substituted into the target characteristic formula of the Taguchi method, such as Equations (1)–(3), and the S/N ratio can be obtained. When you want the value of the quality level to be as large as possible, use Formula (1). When you want the value of the quality level to be as small as possible, use Formula (2). When you want the value of the quality level characteristic to be as close to the target value as possible, use Formula (3). High S/N ratios indicate that the quality of the thin-film coating is more stable. The higher the S/N ratio of the factor, the greater the impact on the target characteristics [39]. In this work, only two types of signal-to-noise ratios are considered, namely, the larger the better and the smaller the better.

Larger-The-Best:

$$SN_{LTB} = -10 \times \log_{10}\left[\frac{1}{n}\sum_{i=1}^{n}\frac{1}{y_i^2}\right] \quad (1)$$

Smaller-The-Best:

$$SN_{STB} = -10 \times \log_{10}\left(\frac{1}{n}\sum_{i=1}^{n} y_i^2\right) \quad (2)$$

Nominal-The-Best:

$$SN_{NTB} = 10 \times \log_{10}\left[\frac{\bar{y}^{-2}}{s^2}\right] \quad (3)$$

3. Results and Discussion

This study employed the Taguchi method in the electron beam evaporation coating process to optimize the process parameters for un-doped and W-doped VO_2 thin films. Our goal was to improve the reliability of the measurements by conducting experiments on three B270 circular glass substrates for each experimental combination. The key metrics measured included surface roughness, residual stress, visible light transmittance, and infrared transmittance. To reduce the measurement error and improve the accuracy of the experimental results, the median of each measurement was calculated, and the arithmetic mean was used as the representative result for each experimental set. By analyzing results from various parameter combinations, we assessed the impact of each process parameter on the quality of the thin films using the Taguchi method. A total of 16 different parameter combinations were designed, and Minitab® statistical software (Version 19.2020.1, Minitab, Ltd., Coventry, UK) was used to compute the signal-to-noise (S/N) ratio for each characteristic index, helping to predict the optimal solution for performance evaluation and process optimization. By analyzing the S/N ratio effect table and the S/N ratio effect plot, it can be seen that the average S/N ratio performance of each level is generally better at levels with larger S/N ratio values than those with smaller S/N ratio values. If the S/N ratio difference between different levels is not significant, it means that there is no significant difference between levels. The greater the difference between the maximum S/N value and the minimum S/N value in each factor, the greater the impact of the factor on the characteristic, and vice versa. The results of the analysis using Minitab software are shown below, and the optimal conditions and sequences that affect W-doped VO_2 film performance were further determined.

For the surface roughness measurement of VO_2 thin films, the measurement size of the film surface roughness was set to 100 μm × 100 μm. The root mean square (RMS) value is the square root of the variance or the standard deviation of the film surface from the reference plane within the sampling area. This value is calculated by a statistical formula with 10 measurements. Figure 3 reveals the surface roughness contours of the VO_2 thin films deposited with different tungsten contents. The RMS surface roughness was 2.47 nm for un-doped VO_2 thin film, 2.12 nm for 3% W-VO_2 film, 2.33 nm for 4% W-VO_2 film, and 2.41 nm for 4% W-VO_2 film. Table 3 is the reaction table of the surface roughness signal-to-noise ratio analysis results, which can provide a clearer and more intuitive understanding of how each process parameter affects the quality of the target film. The influencing factors are film thickness > oxygen flow > VO_2 tungsten doping ratio > heating temperature. The delta statistics are computed based on the difference between the highest and the lowest average value of each factor. Ranks are then assigned according to the delta value. The rank in the response table helps quickly identify which factors have the most impact. The factor with the largest increment value is assigned rank 1, the factor with the second largest increment is assigned rank 2, and so on. The asterisks in Tables 3–6 indicate significance.

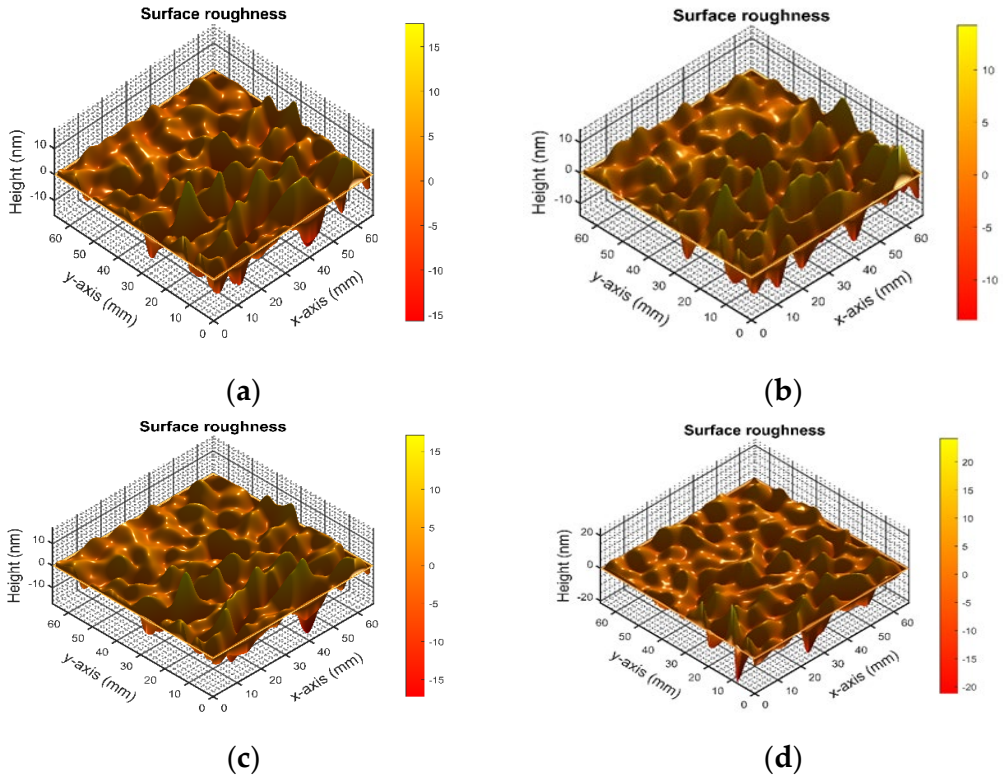

Figure 3. Surface roughness contours of the VO_2 thin films with different tungsten contents (**a**) 0%; (**b**) 3% W; (**c**) 4% W; (**d**) 5% W-doped VO_2.

Table 3. The smaller the S/N ratio, the better the surface roughness performance.

Response Table for Signal-to-Noise Ratios				
Level	**O_2 Flow Rate (sccm)**	**Substrate Temperature (°C)**	**Film Thickness (nm)**	**W Doping Ratio (%)**
1	−6.679	−6.659	* −6.598	−6.639
2	−6.649	−6.639	−6.608	* −6.618
3	−6.649	* −6.628	−6.659	−6.659
4	* −6.598	−6.648	−6.709	−6.659
Delta	0.081	0.031	0.111	0.040
Rank	2	4	1	3

Table 4. The smaller the S/N ratio, the better the residual stress performance.

Response Table for Signal-to-Noise Ratios				
Level	**O_2 Flow Rate (sccm)**	**Substrate Temperature (°C)**	**Film Thickness (nm)**	**VO_2-W Ratio (%)**
1	13.26	13.36	13.17	13.12
2	* 13.57	* 13.53	13.19	13.49
3	13.22	13.37	* 13.76	12.83
4	13.17	12.95	13.11	* 13.78
Delta	0.40	0.58	0.65	0.96
Rank	4	3	2	1

Table 5. The higher the S/N ratio, the better the transmittance in the visible light region.

Response Table for Signal-to-Noise Ratios				
Level	**O_2 Flow Rate (sccm)**	**Substrate Temperature (°C)**	**Film Thickness (nm)**	**VO_2-W Ratio (%)**
1	* 34.55	34.13	* 35.28	33.12
2	32.97	33.70	35.23	33.40
3	34.04	* 34.21	32.85	34.25
4	33.91	33.42	32.11	* 34.69
Delta	1.58	0.79	3.17	1.56
Rank	2	4	1	3

Table 6. The higher the S/N ratio, the better the transmittance in the infrared region.

Response Table for Signal-to-Noise Ratios				
Level	**O_2 Flow Rate (sccm)**	**Substrate Temperature (°C)**	**Film Thickness (nm)**	**VO_2-W Ratio (%)**
1	8.765	8.774	8.113	8.465
2	8.554	8.761	8.316	8.513
3	8.691	8.737	9.074	9.109
4	* 9.252	* 8.990	* 9.759	* 9.175
Delta	0.698	0.253	1.646	0.709
Rank	3	4	1	2

Figure 4 shows the S/N ratio analysis results of surface roughness. Among them, the variability of film thickness is the largest, which means that film thickness is the most important factor affecting the surface roughness after the deposition of vanadium dioxide films. Relatively speaking, the difference in the substrate heating temperature is minimal, indicating that it has little impact on surface roughness. According to the smaller characteristic analysis in Taguchi's method, the optimal operating conditions are A4B3C1D2 (see Table 1), that is, an oxygen flow rate of 60 sccm, a heating temperature of 280 °C, a film thickness of 60 nm, a VO_2-doped tungsten ratio of 3%. According to the Minitab software analysis, the predicted surface roughness is 2.112 nm, the standard deviation is 0.0145, and the S/N ratio is −6.5122. The results show that the minimum surface roughness is 2.12 nm. The prediction is close to the actual situation, which also verifies the effectiveness of the optimal parameter combination in reducing surface roughness. In addition, it was observed in the experiment that as the tungsten doping concentration increases, the surface roughness of the VO_2 film shows a gradually increasing trend. This phenomenon may be due to the uneven distribution of doping atoms caused by higher concentrations of tungsten doping or the introduction of internal stress in the film structure, thereby affecting the growth process of the VO_2 film. The resulting internal structural changes may lead to inhomogeneities in surface topography and an increase in roughness.

Figure 5 shows the S/N ratio analysis results of the residual stress. Among them, the tungsten-doped ratio of VO_2 has the greatest variability, which means that the tungsten-doped ratio of VO_2 films is the most important factor affecting the residual stress after the deposition of vanadium dioxide films. Relatively speaking, the oxygen flow rate has the smallest difference, showing that it has a small impact on residual stress. According to the small characteristic analysis of the Taguchi method, the optimal operating conditions are A2B2C3D4 (see Table 1), that is, an oxygen flow rate of 20 sccm, a heating temperature of 265 °C, a film thickness of 120 nm, a tungsten-doped vanadium of 5% oxygen dioxide (VO_2).

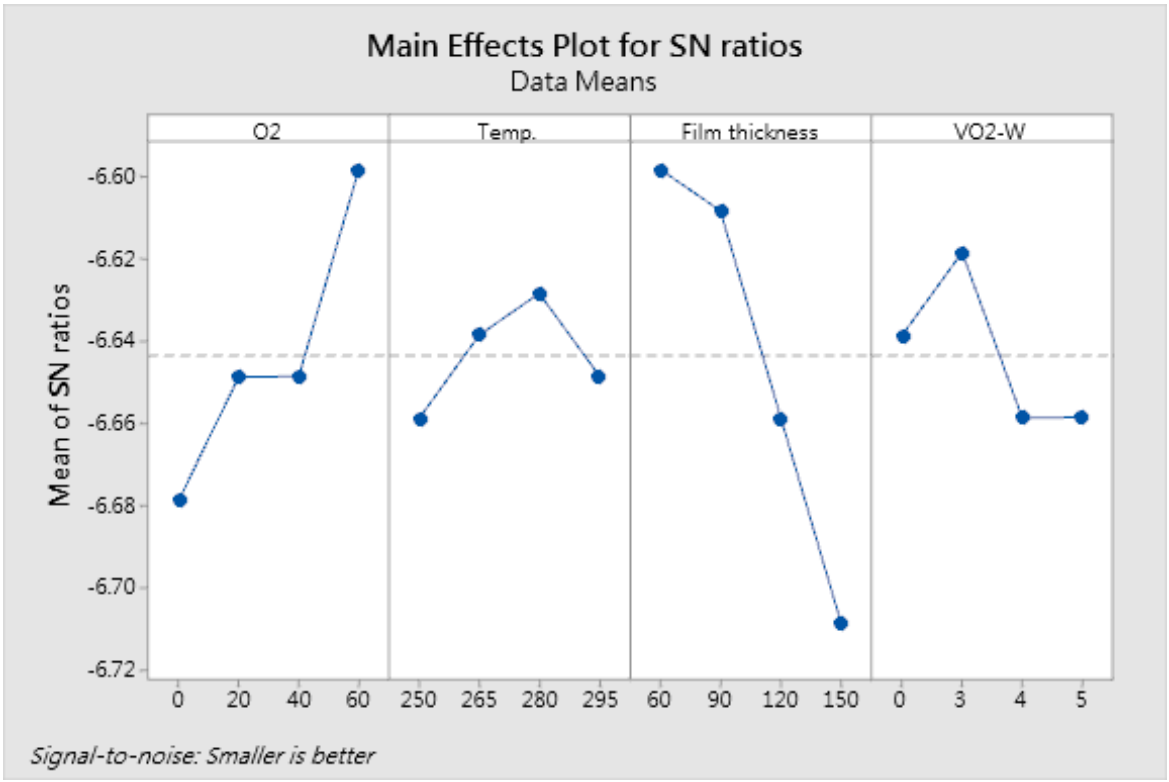

Figure 4. Main effects plot for S/N ratios of surface roughness.

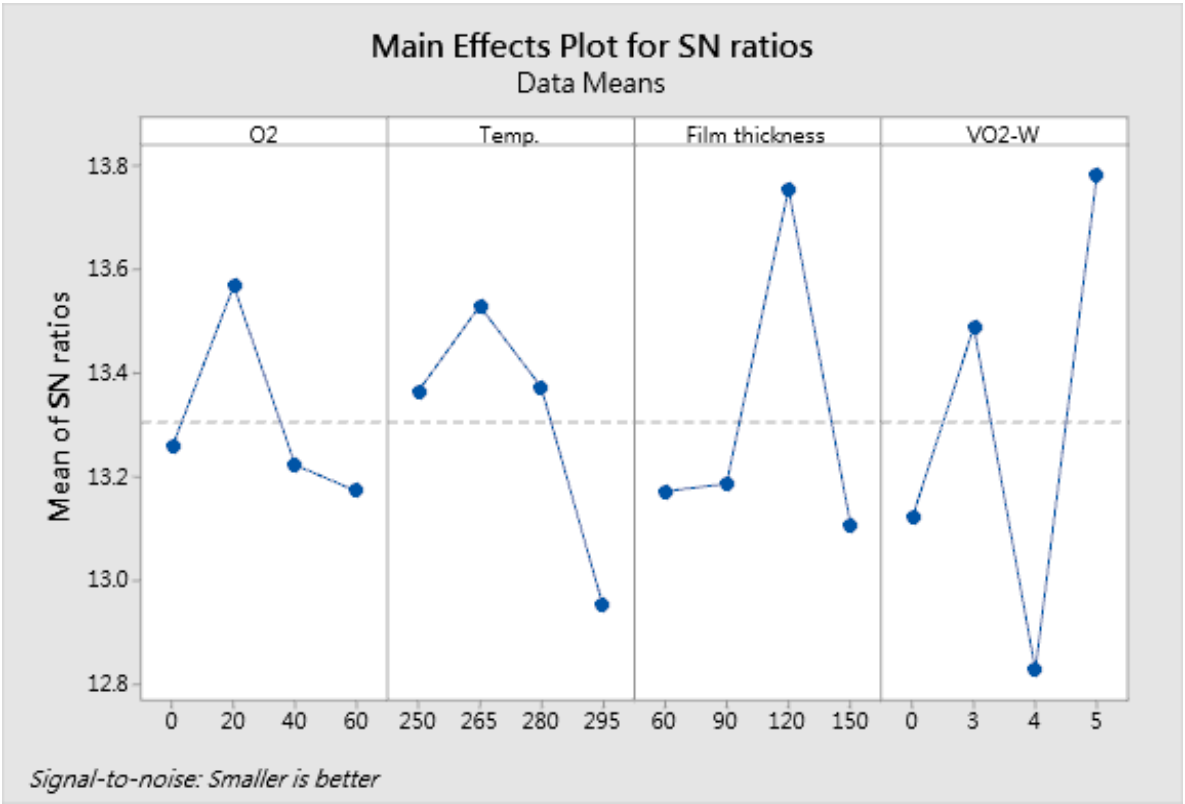

Figure 5. Main effects plot for S/N ratios of residual stress.

As shown in Table 4, the key factors affecting residual stress are the VO_2 tungsten doping ratio > film thickness > heating temperature > oxygen flow rate. Through the Minitab 20 software analysis, the predicted residual stress is −0.182 GPa, the standard deviation is 0.0138, and the S/N ratio is 14.7211. Under these conditions, the VO_2 thin-film sample showed the lowest residual stress of −0.195 GPa for the 5% W-doped VO_2 thin film, and the signal-to-noise ratio is 17.21. It is close to the predicted value, indicating that the optimal parameter combination is in line with expectations in reducing residual stress.

Thin-film surface deformation can be readily obtained by the subtraction of surface contours before and after film deposition, as shown in Figure 6a,b. Thus, the surface profile of the thin film can be reconstructed. By using MATLAB 2023a software analysis, the curvature radius of the B270 glass substrate before the coating was 154.3462 m, with the x-axis and y-axis curvature radii being 145.349 m and 149.768 m, respectively. After the thin-film coating was applied, the glass substrate's curvature radius increased to 186.413 m, with the x-axis and y-axis curvature radii being 178.724 m and 173.153 m, respectively. The residual stress value of −0.195 GPa was measured by a Twyman–Green interferometer. The curvature radius of the glass substrate increases from before coating to after coating, while the PV (peak to valley) value decreases, indicating that the thin film is in a state of compressive stress.

Figure 7 shows the S/N ratio analysis results of visible light transmittance. Among them, the film thickness has the largest variability, which means that film thickness is the most important factor affecting the visible light band transmittance after vanadium dioxide film deposition. Relatively speaking, the difference in heating temperature is the smallest, showing that it has a small impact on the refractive index of the thin film. The optimal operating conditions are A1B3C1D4 (see Table 1), that is, an oxygen flow rate of 0 sccm, a heating temperature of 280 °C, a film thickness of 60 nm, and a VO_2-doped tungsten ratio of 5%.

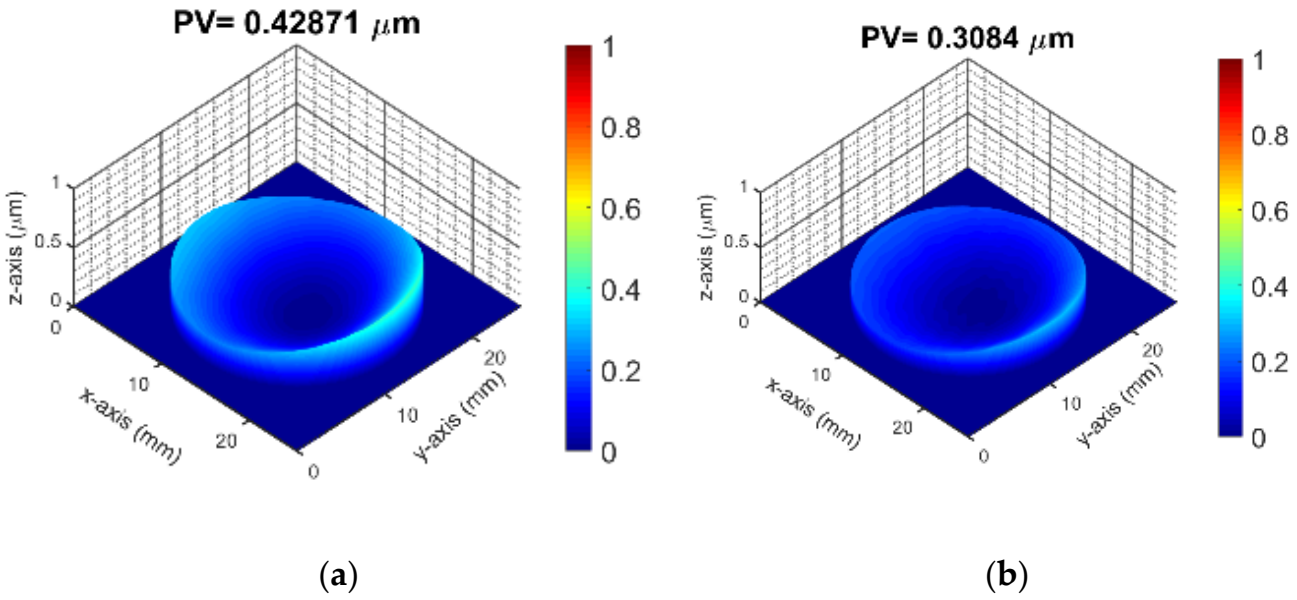

(**a**) (**b**)

Figure 6. The 3D surface profile of the VO_2 thin film coated on B270 glass substrate (**a**) before coating; (**b**) after thin film deposition.

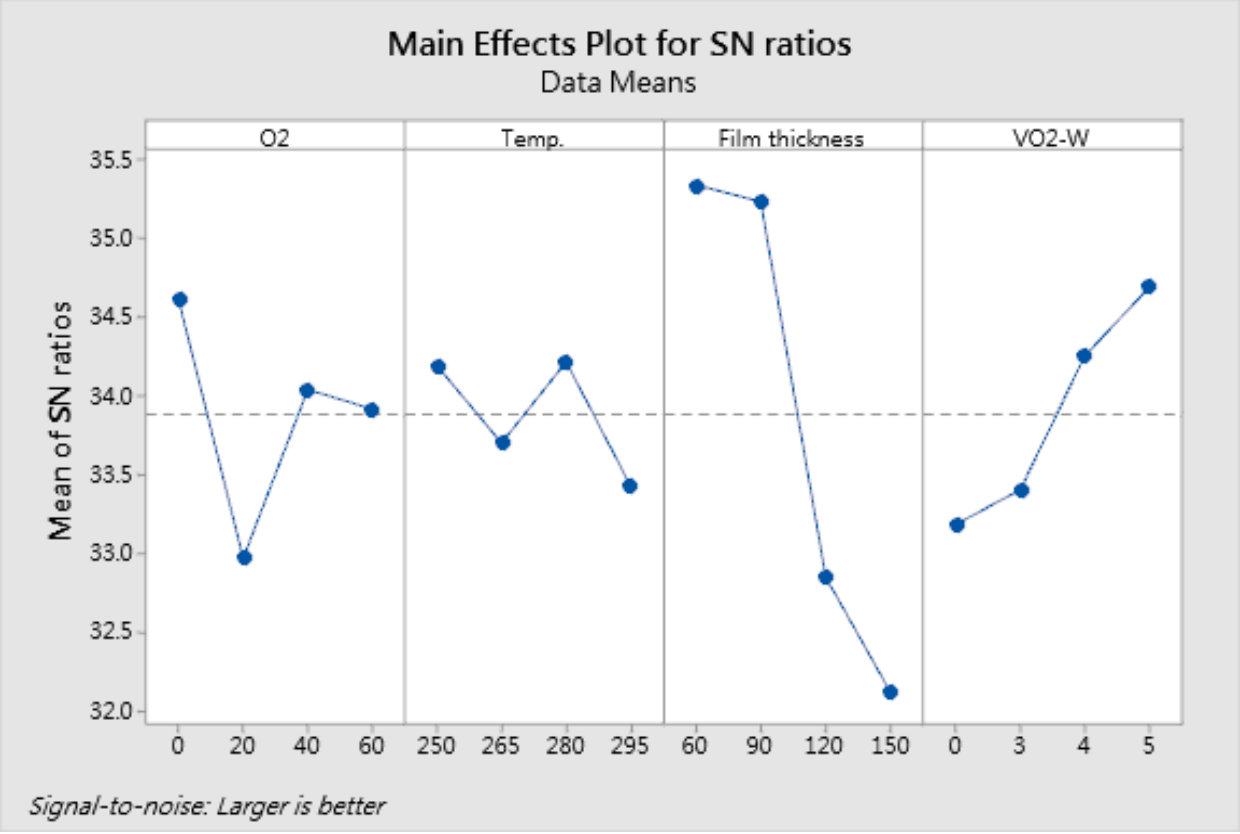

Figure 7. Main effects plot for S/N ratios of visible light transmittance.

It can be seen from Table 5 that the order of key factors affecting the transmittance of the visible light band is film thickness > oxygen flow > VO_2 tungsten doping ratio > heating temperature. According to Minitab 20 software prediction, the average transmittance in the visible light band is 68.09%. The standard deviation is 0.9768, and the signal-to-noise ratio is 37.1298. After experiments, the maximum visible light transmittance is 64.33%, and the signal-to-noise ratio is 36.17. Similarly to the predictions, the optimal parameter combinations are shown to obtain ideal experimental results.

The optimal parameter combination for visible light transmittance is shown in Table 5. It reveals an oxygen flow rate of 0 sccm, a heating temperature of 280 °C, a film thickness of 60 nm, and a 5% tungsten-doped vanadium dioxide (VO_2). Under these conditions, the visible light transmittance of the VO_2 thin film is up to 64.33%.

In addition, we observed that as the W-doping concentration increases, the grain size of the VO_2 thin film shows a gradually increasing trend. This microstructural change may increase film surface roughness, further exacerbating light scattering and reflection effects. Due to the enhancement of light scattering and reflection, the optical transmittance is significantly affected, especially in the visible light band, and the transmission characteristics of the film become more complex.

Figure 8 shows the S/N ratio analysis results of the transmittance in the infrared band. The film thickness has the largest variability, which means that film thickness is the most important factor affecting the infrared transmittance after the deposition of the vanadium dioxide film. Relatively speaking, the difference in heating temperature is the smallest, showing that it has a small impact on the infrared transmittance of thin films. According to the small feature analysis in the Taguchi method, the optimal condition is A4B4C4D4 (see Table 1). As shown in Table 6, the key factors affecting infrared transmittance are film thickness, the VO_2 tungsten doping ratio, oxygen flow rate, and heating temperature. The oxygen flow rate is 60 sccm, the heating temperature is 295 °C, the film thickness is 150 nm, and the VO_2 tungsten doping ratio is 5%. According to the analysis of Minitab 20

software, the average predicted infrared transmittance is 28.38%, the standard deviation is 0.0353, and the S/N ratio is 10.7293. After thin-film coating experiments, the lowest infrared transmittance is 31.34%, and the S/N ratio is 10.08. The prediction is similar to the experimental results, indicating that the optimal parameter combination has achieved the expected results in reducing infrared transmittance.

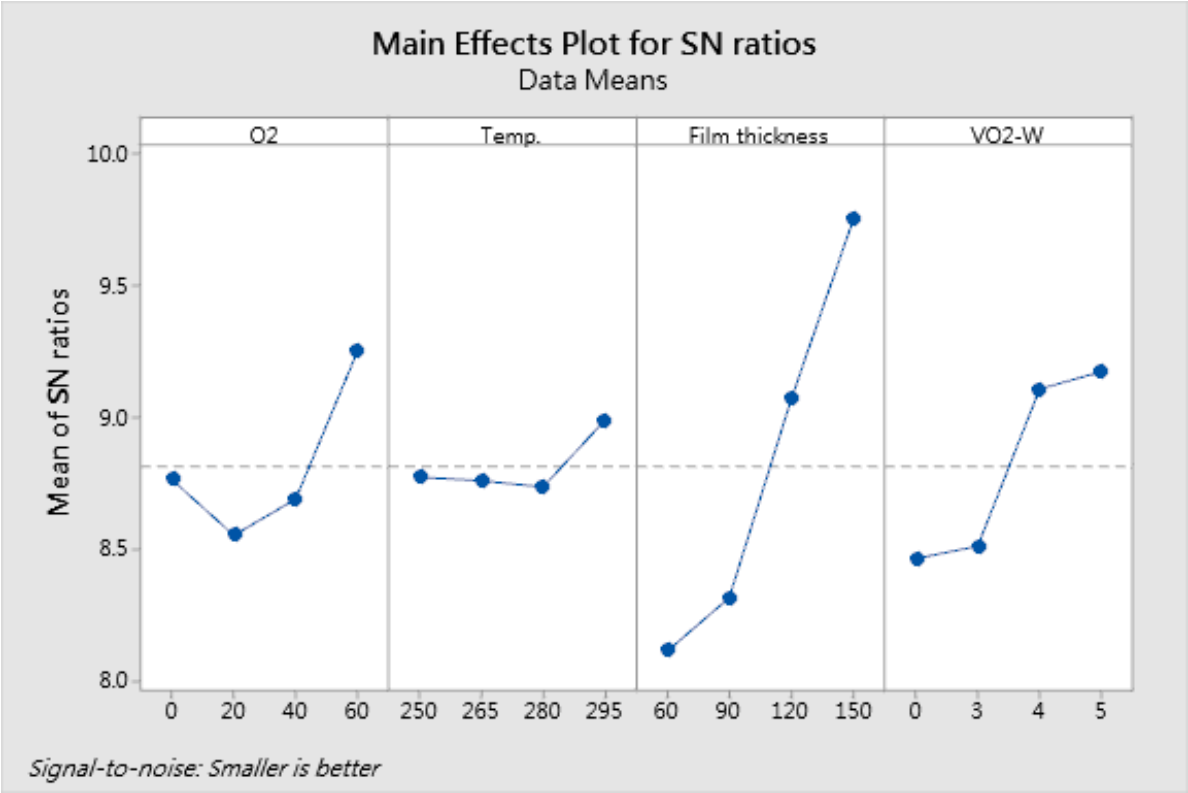

Figure 8. Main effects plot for S/N ratios of infrared transmittance.

Vanadium dioxide-based thermochromic coatings have been widely investigated for use in such smart windows. W-doping VO_2 will be used to decrease the phase transition temperature of VO_2 thin film, of which visible light transmittance will be improved. We compared the visible light transmittance and infrared transmittance of tungsten-doped VO_2 thin films with the literature on their optical properties, as shown in Table 7. At visible light wavelengths, when a thin film transitions from a semiconductor to a metal, the transmittance of light through VO_2 increases, and vice versa. After crossing the wavelength threshold, when the wavelength approaches IR or IR, the transmittance of light through VO_2 begins to decrease as the thin film transitions from semiconductor to metal, and vice versa [40].

Table 7. Comparison of visible light and infrared transmittance for W-doped VO2 thin films.

Coating Technique	Visible Light Transmittance	Infrared Transmittance	References
Sol–gel spin coating	35%	NA	[41]
Thermal oxidation	40–50%	57%	[42]
Spin coating	35%	NA	[43]
DC-reactive magnetron sputtering	54%	59%	[44]
Pulsed laser deposition	62.2%	NA	[45]
Electron beam evaporation with IAD	64.33%	31.34%	This work

4. Conclusions

By applying the Taguchi method, the number of experiments is drastically reduced. A L_{16} (4^4) Taguchi orthogonal array and the signal-to-noise (S/N) ratio were used for the optimization of coating parameters. The signal-to-noise ratio takes into account both mean and variability when assessing the importance of process parameters. This study effectively determined the optimal design parameters to optimize the best performance of VO_2 thin films in terms of high visible light transmittance, low infrared transmittance, low residual stress, and low surface roughness. These findings facilitate the fabrication of high-quality single-layer VO_2 thin films and lay the foundation for future applications in multi-layer composite films or sandwich-structured vanadium dioxide smart windows. Based on experimental design and statistical analysis using the Taguchi method, we systematically investigated the effects of various factors on the performance of VO_2 thin films and identified the optimal process conditions.

The target characteristics of visible light transmittance, infrared transmittance, residual stress, and surface roughness after VO_2 thin-film deposition were discussed. For different target characteristics, the Taguchi method allows us to determine the optimal value of specific parameters for single-objective optimization. The results can be summarized as follows:

1. When the oxygen flow rate is 60 sccm, the heating temperature is 280 °C, the film thickness is 60 nm, and the VO_2 is doped with 3% tungsten, the VO_2 thin film exhibits the lowest surface roughness of 2.12 nm.
2. Under conditions of 20 sccm oxygen flow rate, 265 °C heating temperature, 120 nm film thickness, and 5% tungsten doping, the VO_2 thin film shows the lowest residual stress of −0.195 GPa.
3. Under conditions of an oxygen flow rate of 0 sccm, a heating temperature of 280 °C, a film thickness of 60 nm, and a 5% tungsten doping, the VO_2 thin film achieves the highest visible light transmittance of 64.33%.
4. When the oxygen flow rate is 60 sccm, the heating temperature is 295 °C, the film thickness is 150 nm, and the tungsten doping is 5%, the VO_2 thin film exhibits the lowest infrared transmittance of 31.34%.

In conclusion, by determining these optimal process parameters, we can better control and optimize the performance of VO_2 thin films, thus enhancing their practical value in engineering applications. We have obtained parameter combinations with the best quality properties for single-objective prediction. These optimized parameters can ensure the excellent performance of VO_2 thin films deposited on B270 glass substrate.

Author Contributions: Conceptualization, C.-L.T.; methodology, C.-L.T. and C.-Y.C.; writing—review and editing, C.-L.T. and J.-K.T.; validation, C.-L.T. and C.-Y.C.; formal analysis, J.-K.T. and C.-C.W., data curation, S.-C.L. and C.-C.W. All authors have read and agreed to the published version of the manuscript.

Funding: This research was supported by the National Science and Technology of Council, under project number NSTC 112-2221-E-035-071.

Data Availability Statement: The data are not publicly available due to privacy.

Acknowledgments: The authors are grateful for the Precision Instrument Support Center of Feng Chia University for providing SPM analytical facilities.

Conflicts of Interest: The authors declare no conflicts of interest.

References

1. Shen, N.; Chen, S.; Huang, R.; Huang, J.; Li, J.; Shi, R.; Niu, S.; Amini, A.; Cheng, C. Vanadium dioxide for thermochromic smart windows in ambient conditions. *Mater. Today Energy* **2021**, *21*, 100827. [CrossRef]
2. Jung, K.H.; Yun, S.J.; Slusar, T.; Kim, H.T.; Roh, T.M. Highly transparent ultrathin vanadium dioxide films with temperature-dependent infrared reflectance for smart windows. *Appl. Surf. Sci.* **2022**, *589*, 714–721. [CrossRef]

3. Cui, Y.; Ke, Y.; Liu, C.; Chen, Z.; Wang, N.; Zhang, L.; Zhou, Y.; Wang, S.; Gao, Y.; Long, Y. Thermochromic VO_2 for energy-efficient smart windows. *Joule* **2018**, *2*, 1707–1746. [CrossRef]
4. Jin, P.; Xu, G.; Tazawa, M.; Yoshimura, K. Design, formation and characterization of a novel multifunctional window with VO_2 and TiO_2 coatings. *Appl. Phys. A* **2003**, *77*, 455–459. [CrossRef]
5. Granqvist, C.G. Window coatings for the future. *Thin Solid Film.* **1990**, *193*, 730–741. [CrossRef]
6. Kang, S.K.; Ho, D.H.; Lee, C.H.; Lim, H.S.; Cho, J.H. Actively operable thermoresponsive smart windows for reducing energy consumption. *ACS Appl. Mater. Interfaces* **2020**, *12*, 33838–33845. [CrossRef]
7. Vernardou, D.; Pemble, M.E.; Sheel, D.W. The Growth of Thermochromic VO_2 Films on Glass by Atmospheric-Pressure CVD: A Comparative Study of Precursors, CVD Methodology, and Substrates. *Chem. Vap. Depos.* **2006**, *12*, 263–274. [CrossRef]
8. Gagaoudakis, E.; Aperathitis, E.; Michail, G.; Kiriakidis, G.; Binas, V. Sputtered VO_2 coatings on commercial glass substrates for smart glazing applications. *Sol. Energy Mater. Sol. Cells* **2021**, *220*, 110845. [CrossRef]
9. Zhang, J.; Li, J.; Chen, P.; Rehman, F.; Jiang, Y.; Cao, M.; Zhao, Y.; Jin, H. Hydrothermal growth of VO_2 nanoplate thermochromic films on glass with high visible transmittance. *Sci. Rep.* **2016**, *6*, 27898. [CrossRef]
10. Seyfouri, M.M.; Binions, R. Sol-gel approaches to thermochromic vanadium dioxide coating for smart glazing application. *Sol. Energy Mater. Sol. Cells* **2017**, *159*, 52–65. [CrossRef]
11. Wang, S.; Owusu, K.A.; Mai, L.; Ke, Y.; Zhou, Y.; Hu, P.; Magdassi, S.; Long, Y. Vanadium dioxide for energy conservation and energy storage applications: Synthesis and performance improvement. *Appl. Energy* **2018**, *211*, 200–217. [CrossRef]
12. Vu, T.D.; Chen, Z.; Zeng, X.; Jiang, M.; Liu, S.; Gao, Y.; Long, Y. Physical vapour deposition of vanadium dioxide for thermochromic smart window applications. *J. Mater. Chem. C* **2019**, *7*, 2121–2145. [CrossRef]
13. Marszałek, K.; Winkowski, P.; Marszałek, M. Antireflective bilayer coatings based on AlO film for UV region. *Mater. Sci.-Pol.* **2015**, *33*, 6–10. [CrossRef]
14. Yang, Z.; Ko, C.; Ramanathan, S. Oxide electronics utilizing ultrafast metal-insulator transitions. *Annu. Rev. Mater. Res.* **2011**, *41*, 337–367. [CrossRef]
15. Chang, T.C.; Cao, X.; Bao, S.H.; Ji, S.D.; Luo, H.J.; Jin, P. Review on thermochromic vanadium dioxide based smart coatings: From lab to commercial application. *Adv. Manuf.* **2018**, *6*, 1–19. [CrossRef]
16. Omer, A.M. Energy, environment and sustainable development. *Renew. Sustain. Energy Rev.* **2008**, *12*, 2265–2300. [CrossRef]
17. Green, M.A. Photovoltaics: Technology overview. *Energy Policy* **2000**, *28*, 989–998. [CrossRef]
18. Bhupathi, S.; Wang, S.; Ke, Y.; Long, Y. Recent progress in vanadium dioxide: The multi-stimuli responsive material and its applications. *Mater. Sci. Eng. R Rep.* **2023**, *155*, 100747. [CrossRef]
19. Xu, S.; Ma, H.; Dai, S.; Jiang, Z. Study on optical and electrical switching properties and phase transition mechanism of Mo 6+-doped vanadium dioxide thin films. *J. Mater. Sci.* **2004**, *39*, 489–493. [CrossRef]
20. Lopez, R.; Boatner, L.A.; Haynes, T.E.; Feldman, L.C.; Haglund, R.F. Synthesis and characterization of size-controlled vanadium dioxide nanocrystals in a fused silica matrix. *J. Appl. Phys.* **2002**, *92*, 4031–4036. [CrossRef]
21. Liang, Z.; Zhao, L.; Meng, W.; Zhong, C.; Wei, S.; Dong, B.; Xu, Z.; Wan, L.; Wang, S. Tungsten-doped vanadium dioxide thin films as smart windows with self-cleaning and energy-saving functions. *J. Alloys Compd.* **2017**, *694*, 124–131. [CrossRef]
22. Pan, M.; Zhong, H.; Wang, S.; Liu, J.; Li, Z.; Chen, X.; Lu, W. Properties of VO_2 thin film prepared with precursor VO $(acac)_2$. *J. Cryst. Growth* **2004**, *265*, 121–126. [CrossRef]
23. Ji, H.; Liu, D.; Cheng, H. Infrared optical modulation characteristics of W-doped VO_2 (M) nanoparticles in the MWIR and LWIR regions. *Mater. Sci. Semicond. Process.* **2020**, *119*, 105141. [CrossRef]
24. Harrick, N.J.; Du Pre, F.K. Effective thickness of bulk materials and of thin films for internal reflection spectroscopy. *Appl. Opt.* **1996**, *5*, 1739–1743. [CrossRef] [PubMed]
25. Tien, C.L.; Chiang, C.Y.; Lin, S.C. Optimization of Electron-Beam Evaporation Process Parameters for ZrN Thin Films by Plasma Treatment and Taguchi Method. *Plasma* **2023**, *6*, 478–491. [CrossRef]
26. Dehnad, K. *Quality Control, Robust Design, and the Taguchi Method*; Springer Science & Business Media: Berlin, Germany, 2012.
27. Barker, T.B. *Engineering Quality by Design: Interpreting the Taguchi Approach*; CRC Press: Boca Raton, FL, USA, 1990; Volume 113.
28. Swanepoel, R. Determination of the thickness and optical constants of amorphous silicon. *J. Phys. E Sci. Instrum.* **1983**, *16*, 1214–1222. [CrossRef]
29. Panjan, P.; Drnovšek, A.; Gselman, P.; Čekada, M.; Panjan, M. Review of growth defects in thin films prepared by PVD techniques. *Coatings* **2020**, *10*, 447. [CrossRef]
30. Lukaszkowicz, K. Review of nanocomposite thin films and coatings deposited by PVD and CVD technology. In *Nanomaterials*; InTech: Houston, TX, USA, 2011; pp. 145–163.
31. Tien, C.L.; Yang, H.M.; Liu, M.C. The measurement of surface roughness of optical thin films based on fast Fourier transform. *Thin Solid Film.* **2009**, *517*, 5110–5115. [CrossRef]
32. Tien, C.L.; Yu, K.C.; Tsai, T.Y.; Lin, C.S.; Li, C.Y. Measurement of surface roughness of thin films by a hybrid interference microscope with different phase algorithms. *Appl. Opt.* **2014**, *53*, H213–H219. [CrossRef] [PubMed]
33. Tien, C.L.; Lin, T.W.; Yu, K.C.; Tsai, T.Y.; Shih, H.F. Evaluation of electrical, mechanical properties, and surface roughness of DC sputtering nickel-iron thin films. *IEEE Trans. Magn.* **2014**, *50*, 1–4. [CrossRef]
34. Tien, C.L.; Zeng, H.D. Measuring residual stress of anisotropic thin film by fast Fourier transform. *Opt. Express* **2010**, *18*, 16594–16600. [CrossRef]

35. Takeda, M.; Ina, H.; Kobayashi, S. Fourier-transform method of fringe-pattern analysis for computer-based topography and interferometry. *J. Opt. Soc. Am.* **1982**, *72*, 156–160. [CrossRef]
36. Takeda, M.; Mutoh, K. Fourier-transform profilometry for the automatic measurement of 3-D object shapes. *Appl. Opt.* **1983**, *22*, 3977–3982. [CrossRef] [PubMed]
37. Tien, C.L.; Lee, C.C.; Tsai, Y.L.; Sun, W.S. Determination of the mechanical properties of thin films by digital phase shifting interferometry. *Opt. Commun.* **2001**, *198*, 325–331. [CrossRef]
38. Puh, F.; Jurkovic, Z.; Perinic, M.; Brezocnik, M.; Buljan, S. Optimization of machining parameters for turning operation with multiple quality characteristics using Grey relational analysis. *Teh. Vjesn.* **2016**, *23*, 377–382.
39. Krishnaiah, K.; Shahabudeen, P. *Applied Design of Experiments and Taguchi Methods*; PHI Learning Pvt., Ltd.: Delhi, India, 2012.
40. Novodvorsky, A.; Parshina, L.S.; Karamova, O.D. Influence of the conditions of pulsed laser deposition on the structural, electrical, and optical properties of VO_2 thin films. *Semiconductors* **2015**, *49*, 563–569. [CrossRef]
41. Fallah Vostakola, M.; Mirkazemi, S.M.; Eftekhari Yekta, B. Structural, morphological and optical properties of W-doped VO_2 thin films prepared by sol-gel spin coating method. *Int. J. Appl. Ceram. Technol.* **2018**, *16*, 943–950. [CrossRef]
42. Taylor, S.; Chao, J.; Long, L.; Vlastos, N.; Liping Wang, L. Temperature-dependent Optical Characterization of VO_2 Thin Film Prepared from Furnace Oxidation Method. *ES Mater. Manuf.* **2019**, *6*, 62–67. [CrossRef]
43. Al-Douri, Y.; Abd El-Rehim, A.F. Preparation and Investigation of Optical Properties of Tungsten-doped VO_2. *Int. J. Electrochem. Sci.* **2021**, *16*, 211046. [CrossRef]
44. Lyobha, C.J.; Mlyuka, N.R.; Samiji, M.E. Effects of Aluminium and Tungsten Co-Doping on the Optical Properties of VO_2 Based Thin Films. *Tanzan. J. Sci.* **2018**, *44*, 91–99.
45. Bleu, Y.; Bourquard, F.; Barnier, V.; Loir, A.-S.; Garrelie, F.; Donnet, C. Towards Room Temperature Phase Transition of W-Doped VO_2 Thin Films Deposited by Pulsed Laser Deposition: Thermochromic, Surface, and Structural Analysis. *Materials* **2023**, *16*, 461. [CrossRef]